Near-field enhanced ultraviolet resonance Raman spectroscopy using aluminum bow-tie nano-antenna

Ling Li, Shuang Fang Lim, Alexander A. Puretzky, Robert Riehn, and H. D. Hallen

Citation: Appl. Phys. Lett. **101**, 113116 (2012); doi: 10.1063/1.4746747
View online: http://dx.doi.org/10.1063/1.4746747
View Table of Contents: http://apl.aip.org/resource/1/APPLAB/v101/i11
Published by the American Institute of Physics.

Near-field enhanced ultraviolet resonance Raman spectroscopy using aluminum bow-tie nano-antenna

Ling Li,[1] Shuang Fang Lim,[1] Alexander A. Puretzky,[2] Robert Riehn,[1] and H. D. Hallen[1,a)]
[1]*Department of Physics, North Carolina State University, Raleigh, North Carolina 27695-8202, USA*
[2]*Oak Ridge National Laboratory, Oak Ridge, Tennessee 37831-6056, USA*

(Received 23 May 2012; accepted 3 August 2012; published online 13 September 2012)

An aluminum bow-tie nano-antenna is combined with the resonance Raman effect in the deep ultraviolet to dramatically increase the sensitivity of Raman spectra to a small volume of material, such as benzene used here. We further demonstrate gradient-field Raman peaks for several strong infrared modes. We achieve a gain of $\sim 10^5$ in signal intensity from the near field enhancement due to the surface plasmon resonance in the aluminum nanostructure. The on-line resonance enhancement contributes another factor of several thousands, limited by the laser line width. Thus, an overall gain of hundreds of million is achieved. © *2012 American Institute of Physics*.
[http://dx.doi.org/10.1063/1.4746747]

Since the discovery and demonstration of collective electron oscillations on thin metal films[1] and within nanoscale metallic particles,[2] various nanostructures have been used to enhance electric field. In surface enhanced Raman scattering (SERS),[3] metal surfaces with nanosize roughness and metallic colloidal nanoparticles can amplify the inherently small Raman scattering cross section of materials adsorbed onto them. In addition to the field enhancement ability of colloidal nanoparticles in SERS, a metal coated probe tip in tip-enhanced Raman scattering (TERS)[4–7] can also provide spatial information about scattering sites with sub-wavelength resolution. In the near-field measurement of individual nanoparticles' transmission spectra,[8] the line shape of localized surface plasmon resonance (LSPR) agreed well with theory.[9] The electromagnetic coupling effect between metallic nanoparticles was also observed,[8] which contributes to the resonant optical nano-antenna effect[10] by inducing significantly enhanced electric field in the sub-wavelength volume. In addition to the utility of the optical resonance of nano-antennas in Raman spectroscopy, the nano-antenna effect holds promising applications in many fields: enhancing solar harvesting by focusing the strong enhanced light onto a substrate and inducing photocurrent at the nanoscale;[11] manipulating single molecules by using the strong electric field within a split-tip of near-field scanning optical microscope (NSOM);[12] near-field optics components and sources;[13] nanophotolithography.[14]

In this letter, an aluminum bow-tie nano-antenna combined with the resonance Raman (RR) effect is shown to have an extremely good spectral sensitivity to material within the nanoscale volume between the bow-tie gap. In demonstrating this, we find that models for plasmon enhancement tested in near infrared (IR), visible, and near ultraviolet (UV)[15] are valid in the deep-UV, and that this enhancement factor agrees well with reported experimental and theoretical results.[15] Further, we demonstrate that the strong electric field gradients inside the bow-tie gap induce Raman-like peaks for several strong IR modes. This effect was also observed in TERS (Ref. 4) and explained as a result of special selection rules for gradient-field Raman (GFR).[7,16] This ability to drastically amplify the spectral fingerprint in a tightly controlled nanovolume makes aluminum bow-tie nano-antenna a very good candidate for analyzing single UV-absorbing biomolecules at physiological concentration if it can be integrated with micro- or nano-fluidics.[17]

For biosensing and bioimaging, the deep-UV excitation is favorable because many organic molecules such as nucleic acids and proteins show electronic resonance enhancement in this region. Since aluminum's plasmon resonance wavelength is also in this spectral region,[9] aluminum nanostructures have been employed in SERS and TERS studies of biomolecules in the deep-UV region in a non-destructive mode.[18,19] Instead of a scanned single metal coated probe tip in TERS or nanoparticles in SERS, we use metallic nanostructure with a precisely engineered pattern to concentrate the light into a specific sub-wavelength volume with the nano-antenna technique. It is shown to enhance the field more strongly than TERS.[19]

We prepared aluminum nano-antennas on fused silica substrates by electron beam lithography followed by metal liftoff. Fig. 1 shows a single Al bow-tie antenna made of two 20 nm separated equilateral triangles of 100 nm side length and 50 nm thickness. To achieve surface plasmonic coupling between two Al triangles, these geometric parameters were chosen based on the extrapolation of the dependence of localized surface plasmon wavelength on geometry and size from optical antenna simulations and experiments in near-IR, visible, and near-UV.[15] A final oxygen plasma etching was used to eliminate organic contaminants on the fused silica substrate to avoid spectra interference with the sample's spectra. A thin aluminum oxide layer was formed on the antennas during this process.

A tunable (0.25–1.6 μm) picosecond laser system based on a Ti:sapphire laser(Coherent Mira 900) was used for illumination. Raman spectra were acquired using a confocal micro-Raman system based on a triple monochromator (Jobin Yvon Horiba T64000) with a spectral resolution close to 0.74 cm^{-1}. The scattered light was collected through a microscope in backscattering mode using a reflective objective lens (×52, NA 0.65). The input electric field polarization can be rotated using a half waveplate and a polarizer to

a)Electronic mail: Hans_Hallen@ncsu.edu.

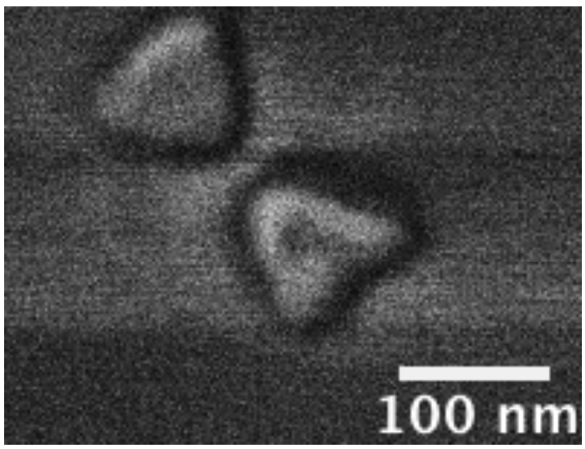

FIG. 1. The SEM image of a 50 nm thick aluminum bow-tie antenna which is formed by two equilateral triangles of 100 nm side length with 20 nm apex to apex gap distance.

have any angular relation with antenna axis defined by the two close triangle apexes. A cylindrical cell made out of teflon was fully filled with pure liquid benzene (CAS# 71432) and covered by the fused silica substrate carrying the bow-tie antennas such that the bow-tie antennas were in contact with the liquid sample. Laser pulses (1–10 pJ/pulse) of 5 ps length with 76 MHz repetition rate at wavelength of 258.8 nm were focused from the substrate side onto one bow-tie antenna.

Fig. 2 shows the resonance Raman spectrum of liquid benzene taken at one antenna site. The 258.8 nm excitation wavelength was not at the peak of the broad absorption band for pure liquid benzene, but within a narrow resonance absorption line of vapor phase benzene (our prior work[19] has found a strong resonance Raman enhancement in liquid benzene at this wavelength). We use values from prior resonance Raman studies[19–21] to assign the measured Raman lines in Gerhard Herzberg notation. The peaks centered at

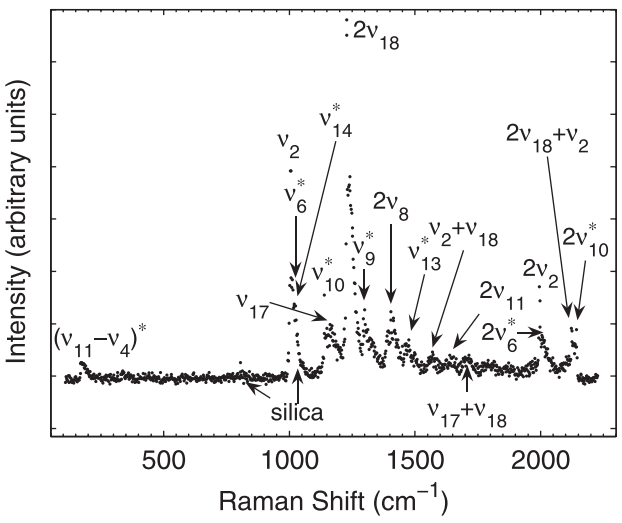

FIG. 2. The resonance Raman spectrum of liquid benzene within the near field of an aluminum bow-tie nano-antenna. The modes indicated by a "∗" are due to gradient-field Raman effect. The laser wavelength was 258.8 nm, the average power was 0.1 mW, the image integration time for one single measurement was 120 s, and the polarization was rotated 27° with respect to the long bow-tie axis which was aligned to the Raman system's default vertical polarization of excitation.

1003, 1160, 1229, 1402, 1570, 1638, 1713, 1994, and 2122 cm^{-1} can be clearly assigned to the total symmetric ring breath mode ν_2, the CH bend mode ν_{17}, the overtones of ring deforming modes $2\nu_{18}$ and $2\nu_8$, the combination of $\nu_2+\nu_{18}$, the overtone of $2\nu_{11}$, the combination of $\nu_{17}+\nu_{18}$, the overtone of ring breath mode $2\nu_2$, and the combination of $2\nu_{18}+\nu_2$, respectively. Note that the overtone modes $2\nu_{18}$ and $2\nu_8$ were strongly enhanced, while their fundamental modes were missing or extremely weak in this spectrum. This was also observed in prior resonance Raman studies of benzene,[19–21] in which the fundamental modes appeared in non-resonance Raman spectra instead of resonance Raman spectra.

Other lines not observed in the prior resonance Raman of benzene are attributed to two factors. The first factor was the interference from fused silica substrate, which gave a weak peak close to 806 cm^{-1} and another one around 1050 cm^{-1},[22] broadening the adjacent Raman line. The second factor is the GFR effect.[7,16] This generates Raman-like peaks from strong IR vibration modes in the vicinity of metallic structures. GFR arises from the abnormally large electric field gradient near a metal surface. Selection rules are obtained by expanding the dipole operator in the vibration coordinate.[7,16] The GFR mechanism explains new spectra lines for allowed IR absorption modes in studies of benzene utilizing SERS,[23] which also gave several orders of magnitude enhancement and a strong electric gradient near the metallic structure surfaces, and has been tested as a function of metal-molecule distance using TERS.[5] The two IR modes at 1012 cm^{-1}(ν_6^*) and 1024 cm^{-1}(ν_{14}^*) gave the broadening effect to the Raman line of ν_2. Similarly, the broadened shape of the line of $2\nu_2$ mode was due to the IR mode of 2006 cm^{-1}($2\nu_6^*$). The feature at 171 cm^{-1} can also be attributed to this effect. A feature with this energy was observed as one of four maximums in the far infrared absorption measurement of liquid benzene and interpreted as a difference spectroscopic effect between the Raman line 849 cm^{-1}(ν_{11}) and the IR line 673 cm^{-1}(ν_4) because no absorption features found in vapor or very thin liquid benzene layer.[24] Other vibrations with IR features can be found at peak centered at 1140 cm^{-1}(ν_{10}^*), 1299 cm^{-1}(ν_9^*), 1474 cm^{-1}(ν_{13}^*), and 2141 cm^{-1}($2\nu_{10}^*$).

The enhancement effect introduced by the LSPR was verified by comparing the micro-Raman measurements taken from the bow-tie antenna site and off the antenna site, Fig. 3. When the whole bow-tie antenna was laterally moved out of the focal spot of the illumination laser, only the strongest peak around 1171 cm^{-1} of the benzene Raman spectrum can be distinguished above the background noise. When the excitation was focused onto the gap of bow-tie antenna, the Raman peaks were clearly observed. Note that this spectrum differs from the one in Fig. 2. The difference can be attributed to photochemical processes which probably produced either stable or unstable benzene derivatives.[25,26] The excitation in Fig. 3 was focused into a small volume of strongly absorbing liquid sample that was static throughout this experiment. The data shown in Fig. 2 were taken with the antenna in liquid, which allowed free diffusive flow. This spectrum in Fig. 3 and that in Fig. 2 do share similar spectral features in the 1000–2100 cm^{-1} region. These vibrations are

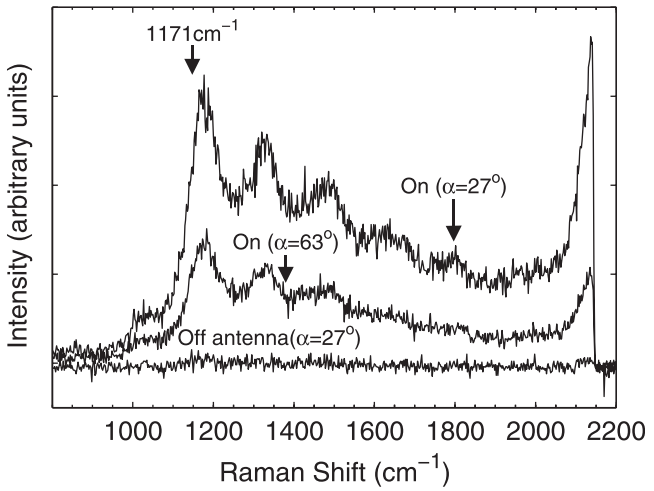

FIG. 3. The excitation-power normalized spectra from repeated measurements. The top spectrum was taken when antenna was in the focused laser spot. The middle one was also taken from a bow-tie site with a different polarization angle. The bottom spectrum was measured after moving the focus spot laterally to a region without bow-tie nano-antenna. The polarization was rotated an angle of α from the long bow-tie axis. The laser wavelength was 258.8 nm. The excitation power used was in the range of 0.05–0.13 mW. The image integration time was 120 s.

evidently not altered strongly by the damage process. Since these spectra can be attained repeatedly by moving the antenna in or out of laser focus, these differences in the spectra do not hinder the demonstration of near-field enhancement of Raman signal from the aluminum bow-tie nano-antenna.

The measured Raman intensity for the spectrum taken at bow-tie antenna site (I_{BT}) had contributions from both LSPR enhanced intensity (let I_{LSPR} be the intensity with only LSPR enhancement) and RR intensity (I_{RR} for only resonance Raman enhancement), while the spectrum taken off bow-tie antenna site ($I_{w/oBT}$) was pure RR intensity. The integrated areas under the peak at 1171 cm^{-1}(depolarized ν_{17} mode) with depolarization ratio of 0.75 ± 0.07 (Ref. 27) of the two spectra were compared to estimate the LSPR enhancement factor. From a calibration test on fused silica, using the polarized Raman line at 483 cm^{-1},[22] the ratio of vertical to horizontal polarization spectrometer throughput efficiency was estimated to be 4.

In order to estimate the LSPR enhancement factor, we also need to know the effective detection volumes probed by normal RR and LSPR enhanced near-field. The 258.8 nm excitation was focused by the objective with NA 0.65 to a diffraction limited spot with diameter of ~500 nm. Half the depth-of-focus can be approximated to be 306 nm, which is smaller than the absorption depth of the illumination in the liquid sample.[19] A cylindrical volume having these two parameters is used as the volume detected by normal RR(V_{RR}), which is estimated to be 6.0×10^7 nm^3, Fig. 3(c). Bow-tie antennas have been shown in previous experimental and theoretical works to confine light in a subwavelength volume between the gap,[15,28] it is safe to assume the probe volume for LSPR enhanced Raman (V_{LSPR}) was a cylindrical volume of $\pi \times (20\,\text{nm})^2 \times 50\,\text{nm} \approx 6.3 \times 10^4$ nm^3, Fig. 3(b). The bow-tie antenna volume ($V_{BT} \approx 4.3 \times 10^5$ nm^3) and V_{LSPR} should be excluded from V_{RR} to account for the probe volume of pure RR when antenna presented. From all considerations above, it can be deduced that

$$I_{BT} = \frac{1}{5}(4 \times 0.25 + 0.75) I_{LSPR} \cos^2\alpha + I_{w/oBT} \frac{V_{RR} - V_{BT} - V_{LSPR}}{V_{RR}},$$

$$I_{w/oBT} = \frac{1}{5}(4 \times 0.25 + 0.75) I_{RR} \cos^2\alpha + \frac{1}{5}(4 \times 0.75 + 0.25) I_{RR} \sin^2\alpha.$$

where $\frac{4}{5}$ and $\frac{1}{5}$ are the normalized spectrometer throughput efficiencies for vertical and horizontal polarization. 0.75 is the Raman depolarization ratio of the peak at 1171 cm^{-1}, 0.25 is then the ratio for intensity scattered in the same direction as incident. α is the angle between incident electric field and the bow-tie axis (aligned to the Raman system's default vertical polarization of excitation). In the field enhanced volume, the density of Raman intensity was $\left[I_{BT} - \frac{I_{w/oBT}(V_{RR} - V_{BT} - V_{LSPR})}{V_{RR}}\right] / 0.35 V_{LSPR} \cos^2\alpha$, and the Raman intensity density in RR volume was I_{RR}/V_{RR}. When $\alpha = 27°$, the largest (smallest) measured ratio for the area of the peak at 1171 cm^{-1} was $I_{BT}/I_{w/oBT} = 201(12)$, corresponding to the LSPR enhancement factor of 2.8×10^5 (0.2×10^5). The statistical result for LSPR enhancement factor is $(3.3 \pm 2.9) \times 10^4$. The relatively large error reflects the various uncertainties and assumptions in the volumes, etc. However, this LSPR enhancement factor implies that the ratio between near-field enhanced Raman intensities with different polarization angles $\frac{I_{BT}(\alpha=27°)}{I_{BT}(\alpha=63°)}$ should be 2.96, which agrees well with the measured peak intensity ratio of 2.3 as shown in Fig. 3. Qualitatively, the average LSPR enhancement is similar to that from direct field measurement in the vicinity of an aluminum bow-tie antenna by NSOM (Ref. 15) and other works on different antennas.[15] Our relative smaller LSPR enhancement factor could be due to aluminum oxidation, which can change the antenna's resonance wavelength.[15] The agreement between our deep UV result and others at longer wavelength indicates that the wavelength scaling for structure size at resonance is still valid in the deep UV.

We have studied, with models and measurements, damage thresholds for the antenna, to have a deeper understanding of the working condition required for a sensitive and repeatable sample analysis. These will be published elsewhere.[29] Methods to alleviate damages to the sample and measurements of relationship between Raman signal intensity and excitation power will be the subject of further study.

In summary, we have achieved a combination of the UV-resonance Raman effect in a liquid sample and deep-UV-driven localized surface plasmon resonance in our aluminum bow-tie nano-antenna. We showed that antenna structure size for the deep-UV plasmon enhancement does extrapolate from simulations and measurements conducted in other wavelengths. The localized surface plasmon resonance effect of the nano-antenna enhanced the Raman signal

from liquid benzene. Additional GFR spectral features at both IR like modes and non-IR modes are due to the strong near-field electric field gradient in the bow-tie gap. These abilities of an aluminum bow-tie nano-antenna can be used to dramatically enhance weak Raman signal when only a small volume of molecules are present such as in nano-fluidic devices. The use of deep UV makes this technique widely applicable, as many biological molecules have electronic resonances in that region.

We would like to thank National Institutes of Health for funding this research (Grant No. R21CA132075). This research was conducted at the Center for Nanophase Materials Sciences, which is sponsored at Oak Ridge National Laboratory by the Scientific User Facilities Division, Office of Basic Energy Sciences, U.S. Department of Energy.

[1]R. H. Ritchie, Phys. Rev. **106**, 874 (1957); A. Otto, Z. Phys. A: Hadrons Nucl. **216**, 398 (1968).
[2]U. Kreibig and P. Zacharias, Z. Phys. A: Hadrons Nucl. **231**, 128 (1970).
[3]T. Vo-Dinh, Trends Analyt. Chem. **17**, 557 (1998).
[4]C. Jahncke, M. Paesler, and H. Hallen, Appl. Phys. Lett. **67**, 2483 (1995).
[5]E. Ayars and H. Hallen, Appl. Phys. Lett. **76**, 3911 (2000).
[6]R. Stockle, Y. Suh, V. Deckert, and R. Zenobi, Chem. Phys. Lett. **318**, 131 (2000).
[7]H. Hallen, NanoBiotechnology **3**, 197 (2007).
[8]T. Klar, M. Perner, S. Grosse, G. von Plessen, W. Spirkl, and J. Feldmann, Phys. Rev. Lett. **80**, 4249 (1998).
[9]M. Vollmer and U. Kreibig, Springer Ser. Mater. Sci. **25**, 26 (1995).
[10]R. Grober, R. Schoelkopf, and D. Prober, Appl. Phys. Lett. **70**, 1354 (1997); K. Crozier, A. Sundaramurthy, G. Kino, and C. Quate, J. Appl. Phys. **94**, 4632 (2003); P. Mühlschlegel, H. Eisler, O. Martin, B. Hecht, and D. Pohl, Science **308**, 1607 (2005).
[11]J. Hsu, E. Fitzgerald, Y. Xie, and P. Silverman, Appl. Phys. Lett. **65**, 344 (1994); J. Wu, F. Chen, Y. Hsiao, F. Chien, P. Chen, C. Kuo, M. Huang, and C. Hsu, ACS Nano **5**(2), 959–967 (2011).
[12]B. Clark III, M. Taylor, and H. Hallen, J. Vac. Sci. Technol. B **28**, 687 (2010).
[13]W. Barnes, A. Dereux, and T. Ebbesen, Nature **424**, 824 (2003); E. Cubukcu, E. Kort, K. Crozier, and F. Capasso, Appl. Phys. Lett. **89**, 093120 (2006).
[14]A. Sundaramurthy, P. Schuck, N. Conley, D. Fromm, G. Kino, and W. Moerner, Nano Lett. **6**, 355 (2006).
[15]P. Schuck, D. Fromm, A. Sundaramurthy, G. Kino, and W. Moerner, Phys. Rev. Lett. **94**, 17402 (2005); G. Chan, J. Zhao, G. Schatz, and R. Duyne, J. Phys. Chem. C **112**, 13958 (2008); H. Fischer and O. Martin, Opt. Express **16**, 9144 (2008); A. Mohammadi, V. Sandoghdar, and M. Agio, J. Comput. Theor. Nanosci. **6**, 2024 (2009); L. Zhou, Q. Gan, F. Bartoli, and V. Dierolf, in *International Quantum Electronics Conference* (Baltimore Optical Society of America, 2009).
[16]E. Ayars, H. Hallen, and C. Jahncke, Phys. Rev. Lett. **85**, 4180 (2000).
[17]J. Tegenfeldt, C. Prinz, H. Cao, R. Huang, R. Austin, S. Chou, E. Cox, and J. Sturm, Anal. Bioanal. Chem. **378**, 1678 (2004); S. Park, Y. Huh, H. Craighead, and D. Erickson, Proc. Natl. Acad. Ssi. U.S.A. **106**, 15549 (2009).
[18]T. Dörfer, M. Schmitt, and J. Popp, J. Raman Spectrosc. **38**, 1379 (2007).
[19]A. Taguchi, N. Hayazawa, K. Furusawa, H. Ishitobi, and S. Kawata, J. Raman Spectrosc. **40**, 1324 (2009); A. Willitsford, Ph.D. dissertation, Pennsylvania State University, 2008; C. Chadwick, Ph.D. dissertation, North Carolina State University, 2009.
[20]L. D. Ziegler and B. Hudson, J. Chem. Phys. **74**, 982 (1981).
[21]S. Asher and C. Johnson, J. Phys. Chem **89**, 1375 (1985); A. Willitsford, C. Chadwick, H. Hallen, S. Kurtz, and C. Philbrick, "Resonance enhanced Raman scattering in liquid benzene at vapor-phase absorption peaks" (unpublished); "Resonance enhanced Raman scattering of ν_9 and ν_{10} b_{2u} vibrational modes in the $^1B_{2u}$ absorption band of benzene" (unpublished).
[22]M. Tobin and T. Baak, J. Opt. Soc. Am. **58**, 1459 (1968).
[23]M. Moskovits and D. P. DiLella, J. Chem. Phys. **73**, 6068 (1980); P. Lund, R. Smardzewski, and D. Tevault, Chem. Phys. Lett. **89**, 508 (1982).
[24]R. Barnes, W. Benedict, and C. Lewis, Phys. Rev. **47**, 129 (1935).
[25]Y. Tsuboi, K. Hatanaka, H. Fukumura, and H. Masuhara, J. Phys. Chem. **98**, 11237 (1994).
[26]J. Pola, M. Urbanova, Z. Bastl, Z. Plzak, J. Subrt, V. Vorlicek, I. Gregora, C. Crowley, and R. Taylor, Carbon **35**, 605 (1997).
[27]T. Ebata, M. Hamakado, S. Moriyama, Y. Morioka, and M. Ito, Chem. Phys. Lett. **199**, 33 (1992).
[28]D. Fromm, A. Sundaramurthy, P. Schuck, G. Kino, and W. Moerner, Nano Lett. **4**, 957 (2004).
[29]Ling Li, Shuang Fang Lim, Alexander A. Puretzky, Robert Riehn, and H. D. Hallen, "The signal intensity of near-field enhanced UV resonance Raman spectroscopy using aluminum bow-tie nano-antenna" (unpublished).